Macroscopic Klein tunneling in spin-orbit-coupled Bose-Einstein condensates

Dan-Wei Zhang,[1,2] Zheng-Yuan Xue,[1] Hui Yan,[1] Z. D. Wang,[2,*] and Shi-Liang Zhu[1,†]

[1]*Laboratory of Quantum Information Technology and School of Physics and Telecommunication Engineering, South China Normal University, Guangzhou 510006, China*

[2]*Department of Physics and Center of Theoretical and Computational Physics, The University of Hong Kong, Pokfulam Road, Hong Kong, China*

(Received 11 April 2011; published 19 January 2012)

We propose an experimental scheme to detect macroscopic Klein tunneling with spin-orbit-coupled Bose-Einstein condensates (BECs). We show that a nonlinear Dirac equation with tunable parameters can be realized with such BECs. Through numerical calculations, we demonstrate that macroscopic Klein tunneling can be clearly detected under realistic conditions. Macroscopic quantum coherence in such relativistic tunneling is clarified and a BEC with a negative energy is shown to be able to transmit transparently through a wide Gaussian potential barrier.

DOI: 10.1103/PhysRevA.85.013628 PACS number(s): 03.75.Mn, 03.65.Pm, 03.75.Lm, 71.70.Ej

I. INTRODUCTION

Shortly after the relativistic equation of electron was established by Dirac, Klein used it to study electron scattering by a potential step and found that there exists a nonzero transmission probability even though the potential height tends to infinity [1], in contrast to the scattering of a nonrelativistic particle. This phenomenon has been referred to as Klein tunneling (KT). KT is an intrinsic relativistic effect and is interpreted as a fundamental property of the Dirac equation, that particle and antiparticle states are inherently linked together as two components of the same spinor wave function [2].

This unique scattering process has attracted lots of interest over the past 80 years but failed to be directly tested by elementary particles due to the requirements for currently unavailable electric field gradients [3]. Interestingly, the dynamics of particles in some systems, such as electrons in graphene [3] and trap ions [4,5], may be described by effective relativistic wave equations and have been proposed for observation of such relativistic tunneling. Ultracold atoms in optical lattices [6] and light-induced gauge fields [7] are also able to behave as relativistic particles [8,9]. Recent experiments in graphene heterojunctions [10,11] have provided some indications for KT. However, the existence of disorders and interactions in these solid-state systems makes it hard to realize full ballistic scatterings. In addition, it seems hard to unambiguously observe KT in graphene since it is a typical two-dimensional (2D) system, while scattering in a 2D system is a combination of perfect transmission for normally incident particles (a relativistic effect) and exponential decay tunneling for obliquely incident particles (a nonrelativistic effect). Moreover, KT as well as the Zitterbewegung effect have been experimentally simulated with trapped ions. [5]

In this paper we propose a feasible experimental scheme for observation of macroscopic KT with spin-orbit-coupled BECs [12,13]. We demonstrate that a 1D nonlinear Dirac equation (NLDE) with tunable parameters can be realized with a spinor BEC in the presence of a light-induced gauge field. Through numerical simulations, we demonstrate that macroscopic KT can be observed under realistic conditions. The simple configuration of a gauge field, in combination with controllable dimensions, interactions, and potential barriers, may provide us with a clean and tunable platform for investigation of interesting relativistic tunneling effects.

We investigate the relativistic tunneling of a macroscopic quantum object by comparing the transmission coefficients between a BEC in the absence of interactions and an incoherent ensemble average of noncondensed atoms. In addition, we find that a realistically weak interaction between atoms slightly affects the transmission coefficients. The main feature of a BEC is that all atoms in the BEC are in the same state and in the same phase and thus the BEC can be considered a macroscopic object. So the tunneling of a BEC we study is the coherent scattering of a macroscopic object. Tunneling in the former shows a distinct difference in relativistic effects between macroscopic objects and the ensemble average of some microscopic particles, while KT has been studied previously only within a single-particle scenario. We also present another unexpected result: that a BEC with a negative energy can almost completely transmit through a Gaussian barrier. Since KT is a relativistic phenomenon associated with an antiparticle in the potential, our proposed spin-orbit-coupled BEC can mimic a macroscopic "anti-BEC" (a superatom made from "antiatoms"), at least in a scattering problem. Therefore, the mimicked anti-BEC may open the possibility of exploring exotic relativistic effects of a macroscopic body (even for very large antimatter), in contrast to the conventional wisdom that relativistic effects are only clear for a microscopic particle.

The paper is organized as follows. In Sec. II we propose an approach to realize a spin-orbit-coupled atomic gas through a Λ-level configuration and then demonstrate that the dynamics of the atoms should be described by the NLDE when the atoms are condensed into a BEC. In Sec. III we show that the region for KT of a single atom can be reached in experiments. Then we demonstrate in Sec. IV that KT of BECs can be clearly observed. We also clarify the macroscopic quantum coherence in such relativistic tunneling and show that a wide Gaussian potential barrier is transparent for a BEC with a negative energy. In Sec. V, we present our discussion and

*zwang@hku.hk
†slzhu@scnu.edu.cn

conclusion. In the Appendix, we briefly review the numerical method to calculate the transmission coefficient of a single atom scattered by a Gaussian potential.

II. REALIZATION OF A NONLINEAR DIRAC EQUATION WITH COLD ATOMS

The Dirac equation with tunable parameters can be realized with ultracold atoms through two approaches [6,8,9]. Similarly to graphene, it was proposed that low-energy quasiparticles in a honeycomb optical lattice should also be described by the relativistic Dirac equation [6]. On the other hand, the Hamiltonian of cold atoms (without optical lattices) with a certain spin-orbit coupling, which can be achieved with synthetic gauge fields, is a Dirac Hamiltonian when the wave number of the atoms is much smaller than the wave number of the laser beams. It is demonstrated that the required spin-orbit coupling can be realized though a tripod-level configuration [8,9]. In this paper we propose that a Λ-level configuration is also feasible for use in the realization of the Dirac equation.

Let us consider the motion of bosonic atoms with mass m in the y-z plane, with each having a Λ-level structure interacting with laser beams as shown in Fig. 1. The ground states $|1\rangle$ and $|2\rangle$ are coupled to an excited state $|3\rangle$ through laser beams characterized, respectively, with the Rabi frequencies $\Omega_1 = \Omega\cos(\kappa_y y)e^{-i\kappa_z z}$ and $\Omega_2 = \Omega\sin(\kappa_y y)e^{i(\pi-\kappa_z z)}$, where $\Omega = \sqrt{|\Omega_1|^2 + |\Omega_2|^2}$. As shown in Fig. 1(b), the Rabi frequencies Ω_1 and Ω_2 can be realized, respectively, with a pair of lasers $\Omega_{1\pm} = \frac{1}{2}\Omega\exp[i(-\kappa_z z \pm \kappa_y y)]$ and $\Omega_{2\pm} = \frac{1}{2}\Omega\exp\{i[-\kappa_z z \pm (\kappa_y y + \pi/2)]\}$, where $\kappa_y = \kappa\cos\varphi$ and $\kappa_z = \kappa\sin\varphi$, with κ being the wave number of the lasers and φ being the angle between the laser and the y axis. The Hamiltonian of a single atom reads $H = \frac{\mathbf{p}^2}{2m} + V(\mathbf{r}) + H_I$, where $V(\mathbf{r}) = \sum_{j=1}^{3}[V_T(\mathbf{r}) + V_b(\mathbf{r})]|j\rangle\langle j|$ denotes the full external potentials (including the trapping potentials V_T and the scattering potential V_b) and the interaction Hamiltonian $H_I = \hbar\Delta|3\rangle\langle 3| - (\sum_{j=1}^{2}\hbar\Omega_j|3\rangle\langle j| + \text{H.c.})$, with Δ as the detuning. Diagonalizing H_I yields the eigenvalues $\hbar\{[\Delta - \sqrt{\Delta^2 + 4\Omega^2}]/2, 0, [\Delta + \sqrt{\Delta^2 + 4\Omega^2}]/2\}$. In the large detuning case, the two eigenstates corresponding to the first two eigenvalues span a near-degenerate subspace and can be considered a pseudospin with spin-orbit coupling induced by a gauge potential [7,14]. Under this condition we obtain the effective Hamiltonian

$$H = \frac{p_y^2 + p_z^2}{2m} + v_y\sigma_y p_y + v_z\sigma_z p_z + \gamma_z\sigma_z + V_T + V_b, \tag{1}$$

where $v_y = \frac{\hbar\kappa_y}{m}$, $v_z = \frac{\hbar\kappa_z\Omega^2}{2m\Delta^2}$, and $\gamma_z = \frac{\hbar^2\Omega^2}{4m\Delta^2}[\kappa_y^2 - (1 + \Omega^2/\Delta^2)\kappa_z^2] + \frac{\hbar\Omega^2}{2\Delta}$. In the derivation, we have dropped an irrelevant constant and assumed that the potentials $V(\mathbf{r})$ are spin independent. Furthermore, the atomic gas can well be confined by a 1D optical waveguide along the y axis [9], so we may further restrict our study in the 1D system. Therefore, both tripod- and Λ-level configurations can be used, in principle, in the realization of the Dirac equation. Compared with the tripod configuration [8,9], a large detuning is necessary in the Λ configuration. However, the laser beams are simpler in the Λ-level configuration. Furthermore, the pseudospins in the Λ configuration would be more robust against the collision of atoms since they are constructed by the lowest two dressed states, while the two dark states in the tripod configuration are not the ground states.

We assume that the interaction can be described by an effective 1D interacting strength $g = 2\hbar^2 a_s N/(m l_\perp^2)$, where a_s is the scattering length, N is the particle number, and $l_\perp$ is the oscillator length associated with a harmonic vertical confinement. The interaction between the atoms (per particle) should be much smaller than the confinement frequency (about kHz) [20] and, thus, is also much smaller than Ω (in the megahertz range), therefore the interaction cannot pump the atoms outside of the near-degenerate subspace. Under the condition $p_y \ll \hbar\kappa_y$, we can safely neglect the p_y^2 term. In addition, we assume that the bosonic atoms are condensed into a BEC state. Within the Gross-Pitaevskii formalism, the interacting bosons in the near-degenerate subspace are then effectively described by a 1D NLDE as $i\hbar\partial_t\Psi = H_{\text{ND}}\Psi$ [15], where

$$H_{\text{ND}} = -i\hbar v_y\sigma_y\partial_y + \gamma_z\sigma_z + g\Psi^\dagger\Psi + V_T + V_b, \tag{2}$$

with v_y being the effective speed of light and γ_z the effective rest energy of the cold atoms. It is a remarkable feature that all parameters, v_y, γ_z, and g, can be controlled experimentally, providing us with a tunable platform for exploration of the relativistic quantum effects.

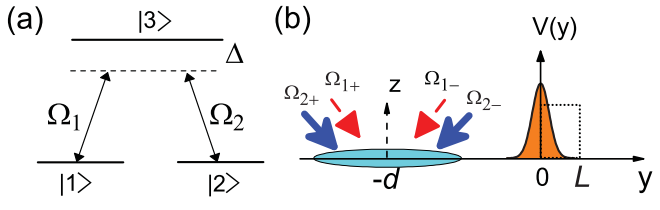

FIG. 1. (Color online) Schematic illustration of the system. (a) Atom with a Λ-level configuration interacting with laser beams characterized by Rabi frequencies Ω_1, Ω_2 and a large detuning Δ. (b) Configuration of laser beams to realize a Dirac-like equation lasers Ω_1 and Ω_2 and an effective Gaussian (square)-shaped potential induced by another laser beam. Atoms are confined in a 1D waveguide along the y axis and scattered by the potential.

III. KLEIN TUNNELING OF A SINGLE ATOM

We now address the relativistic quantum tunneling that can be observed with cold atoms. To get an intuitive physics picture, we first consider a single atom with energy E scattered by a square potential with width L and potential height V_s. Such a potential can be experimentally formed by a laser beam with a flat-top profile [16]. The transmission coefficient T_D for the so-called KT regime, $V_s > E + \gamma_z$ [2], can be obtained explicitly as

$$T_D = [1 + (\eta - \eta^{-1})^2\sin^2(\beta L)/4]^{-1}, \tag{3}$$

where $\eta = \sqrt{\frac{(V_s - E + \gamma_z)(E + \gamma_z)}{(E - V_s + \gamma_z)(\gamma_z - E)}}$ and $\beta = \sqrt{\frac{(V_s - E - \gamma_z)}{(V_s - E + \gamma_z)}}/\hbar$. Compared with the well-known property in nonrelativistic quantum

mechanics that the transmission coefficient decreases monoexponentially with the height V_s or width L, a distinctly different feature within this KT region is that the tunneling amplitude is an oscillation function of V_s or L even when the kinetic energy of the incident particle is less than the height of the barrier. This relativistic effect can be attributed to the fact that the incident particle in a positive energy state can propagate inside the barrier by occupying a negative energy state, which is also a plane wave aligned in energy with that of the particle continuum outside. Matching between positive and negative energy states across the barrier leads to high-probability tunneling. We take the atoms of ^{7}Li as an example. If we choose the practical parameters $\kappa_y = 10^7 \mathrm{m}^{-1}$, $\kappa_z = 0.8 \times 10^7\ \mathrm{m}^{-1}$, $\Omega = 10^7$ Hz, and $\Delta = 10^9$ Hz, it is found that the Klein regime corresponds to the Rabi frequency $\Omega_b^s > 0.162$ MHz, which can be easily achieved in experiments. So we have demonstrated from a simple example that it is feasible to observe KT with cold atoms.

IV. KLEIN TUNNELING OF ATOMIC CONDENSATES

As for a practical experiment, it is required to release two conditions: the trajectory of a single atom is hard to detect, and it is much easier to measure the density evolution of an ensemble of atoms in experiments. Compared with the square potential, a Gaussian potential $V_b^{\mathrm{G}}(y,\nu) = \nu V_{\mathrm{G}} e^{-y^2/\sigma^2}$, where V_{G} is the height and σ characterizes the spatial variance, is much easier to generate. Here ν donates a barrier ($\nu = +$) or a potential well ($\nu = -$), and the potential barrier (well) can be realized by focusing a blue (red)-detuned far-off-resonant Gaussian-shaped laser beam. However, the conditions of resonant transmission vary with the velocity and the width of the potential, and thus both the ensemble of atoms and the Gaussian potential may smooth the oscillations in the transmission coefficient. So it is natural to ask whether KT can still be observed in an ensemble of atoms. Surprisingly, we illustrate below that KT of a BEC may be observed very clearly.

We assume that a BEC consisting of ^{7}Li is initially trapped in a harmonic trap which moves along the y axis. At the initial time $t = 0$, the center of the trap is located at $y = -d$, and the center of the Gaussian potential is at $y = 0$. The trap is turned off at $t = 0$ and then we calculate the evolution of the density profile of the atomic gas after a long enough time for scattering. The single-atom dispersion described in Eq. (2) is characterized by two branches, $E_\pm(k_y) = \pm(\gamma_z^2 + \hbar^2 v_y^2 k_y^2)^{1/2}$, where the lower (upper) branch represents the negative (positive) energy state. One can prepare an initial BEC with a designated mode k_0 at the positive or negative energy branch. The two branches allow us to study a more fruitful tunneling problem: there are four classes of scattering which describe the wave function Ψ_μ [$\mu(=\pm)$] scattered by the potential $V_b^G(y,\nu)$, as shown in Fig. 2(a).

The BEC in a harmonic trap can be well described by a Gaussian wave packet, so we may choose the initial wave function as

$$\Psi_\mu(y,0) = \frac{1}{\sqrt{l_0\sqrt{\pi}}} e^{i\mu k_0 y} e^{-(y+d)^2/2l_0^2} \phi_\mu, \tag{4}$$

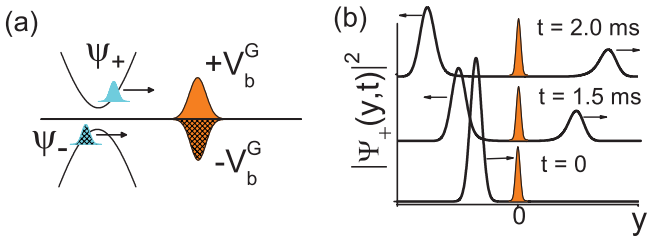

FIG. 2. (Color online) (a) A schematic diagram showing four kinds of scattering events. (b) Normalized density distribution in a scattering process at time $t = 0$, 1.5, and 2.0 ms. The peaks at $y = 0$ are the Gaussian barriers.

where l_0 is the width, k_0 is the central wave number of the wave packet, and the spinors ϕ_μ are defined as $\phi_+ = (i\cos\xi, -\sin\xi)^T$, $\phi_- = (-i\sin\xi, \cos\xi)^T$, with $\xi = \frac{1}{2}\arctan(\hbar v_y k_0/\gamma_z)$ and T the transposition of matrix. This wave function describes a Gaussian wave packet with the central velocity $\hbar(\kappa_y + \mu k_0)/m$ moving along the y axis. After evolution governed by the Dirac-type Eq. (2) with time t, the final wave function becomes

$$\Psi_\mu(y,t) = \hat{\mathcal{T}} \exp\left(-\frac{i}{\hbar}\int_0^t H_{\mathrm{ND}} dt\right) \Psi_\mu(y,0), \tag{5}$$

where $\hat{\mathcal{T}}$ denotes the time ordering operator. We numerically calculate $\Psi_\mu(y,t)$ in Eq. (5) by using the standard split-operator method. According to the method of [19], Eq. (5) can be rewritten as

$$\Psi_\mu(y,t+\delta t) = \left\{e^{-\frac{i}{2\hbar}v_y\sigma_y p_y \delta t} e^{-\frac{i}{\hbar}\gamma_z\sigma_z\delta t} e^{-\frac{i}{\hbar}[V_b^{\mathrm{G}}(y,\nu)+g|\Psi_\mu(y,t)|^2]\delta t} \times e^{-\frac{i}{2\hbar}v_y\sigma_y p_y\delta t} + O(\delta t^3)\right\}\Psi_\mu(y,t). \tag{6}$$

In the sufficiently short time step δt, the high-order term $O(\delta t^3)$ (due to noncommutation) can be safely neglected. Combining with the Fourier transform between the position and the momentum spaces, we can finally get the numerical solution of $\Psi_\mu(y,t)$ following the computation procedure step by step with time step δt.

We have numerically calculated and found the existence of a stationary solution for the scattering process, with an example being shown in Fig. 2(b). After tunneling, the incident wave packet divides into left- and right-traveling wave packets, and only the latter one is on the transmission side of the barrier. Thus we can define the transmission coefficient of the incident wave packet $\Psi_\mu(y,0)$ scattering by a potential $V_b^G(y,\nu)$ as

$$T_{\mu\nu} = \int_\sigma^\infty \Psi_\mu^\dagger(y,\tau)\Psi_\mu(y,\tau)dy. \tag{7}$$

Here τ (being slightly larger than d/v_0) represents a typical time that the reflected and transmitted wave packets are sufficiently away from the Gaussian potential. One can directly measure the transmission coefficient in Eq. (7) since the spatial density distribution $\rho_\mu(y,\tau) = |\Psi_\mu(y,\tau)|^2$ can be detected using absorption imaging [17].

We first look into the tunneling phenomena for a BEC in the absence of interactions ($g = 0$). We note that there are two identities, $T_{++} = T_{--}$ and $T_{-+} = T_{+-}$, since Eq. (2) with

$g = 0$ is invariant under the charge conjugation [18]. We plot the transmission coefficient T_{++} as a function of the height V_G and width σ in Fig. 3(a) with the practical parameters. It is interesting to note that the transmission coefficient decreases exponentially to 0 with V_G when $V_G < V_G^K$, while it increases and then is an oscillating function in the Klein region $V_G > V_G^K$; these results are similar to the results of Eq. (3) for the square barrier. Here the critical value of the potential height may be estimated approximately using the square barrier with $V_G^K = E(k_0) + \gamma_z \approx 0.09$ MHz. Moreover, the feature $T_{++} = T_{--}$ is also confirmed in the inset in Fig. 3(a). As for the transmission coefficient $T_{++}(\sigma)$, we may obtain several tunneling oscillations with the potential width, but it decreases to 0 when the width is further increased. Although the amplitude of tunneling oscillation is less than the unit compared with the tunneling of a single atom, the amplitude of tunneling oscillation can be more than 0.5 and meanwhile the period can be a few micrometers, which is experimentally detectable.

Another interesting feature induced by relativistic effects is that a BEC with negative energy can almost completely transmit a wide Gaussian potential barrier, as shown in Fig. 3(b). The transmission coefficient T_{-+} is an oscillating function of the potential width σ when σ is smaller than 3 μm, while it saturates quickly to the unit when the potential width is larger than 3 μm, leading to the unexpected result that a wide Gaussian potential barrier is actually totally transparent for a BEC. This phenomenon can be understood through the fact that this scattering feature is actually equivalent to that of a BEC of positive energy scattered by a Gaussian potential well because of $T_{-+} = T_{+-}$. We also calculate the transmission coefficient for the central mode of the wave packet, as shown in the inset in Fig. 3(b), which further confirms that a wide enough Gaussian potential well is transparent. The reason lies in the fact that, in contrast to the periodic function (without a saturation value) in a square potential well, the Gaussian potential well is smooth in the whole space and, thus, can even support adiabatic motions of wave packets in the large width limit.

The tunneling properties exhibited in Figs. 3(a) and 3(b) are intrinsic relativistic and macroscopic quantum phenomena that ca not be explained with an incoherent ensemble average of many atoms. To clarify this point, we calculate the average transmission coefficients for an ensemble of N_a noninteracting atoms defined as

$$\langle T \rangle = \frac{1}{N_a} \sum_{i=1}^{N_a} T(k_i), \tag{8}$$

where $T(k_i)$ donates the transmission coefficient for atom i with the wave number k_i scattered by the potential. The numerical calculation method for $T(k_i)$ is given in the Appendix. Here we choose k_i to be the same Gaussian distribution as that of the initial BEC wave function $\Psi_\mu(y,0)$, i.e., $k_i \sim N(k_0, \sigma_k^2)$, with the variance $\sigma_k = 1/l_0$. The $\langle T \rangle$ of 10^4 atoms is shown in the inset in Fig. 3(b), which is almost the same as that of a single atom since σ_k is small. The differences between $\langle T \rangle$ and T_{-+} in Fig. 3(b) demonstrate that the tunneling of BEC is not equivalent to an ensemble average of the individual atoms even with the same distribution of wave number. The coefficient $\langle T \rangle$ represents an incoherent transmission of the individual particles since it is a sum of the transmission coefficients of all particles. In contrast, the phases of all atoms in the BEC are the same and thus the transmission of a BEC is coherent. The coherent transmission in a BEC and incoherence in $\langle T \rangle$ cause the difference in Fig. 3. All particles in the BEC are in the same phase because the macroscopic number of particles is condensed in the same state, so the coherent transmission of the BEC may be called macroscopic quantum tunneling.

To clarify further the macroscopic quantum phenomena in the relativistic tunneling of a BEC, we compare the scaling properties of transmission coefficients for a weakly interacting BEC and an incoherent ensemble average of atoms. An example of scaling of T_{++} is plotted in Fig. 4(a). In the calculations, we have fixed the weak interatomic interaction energy $E_{\rm int} \approx g/l_0$ and kept the parameter $\gamma = mgl_0/N\hbar^2 \ll 1$ [20] for $l_0 = 5$ μm when $N = 10^3$, $l_\perp = 1.4$ μm, and $a_s = 5a_0$ ($\gamma \sim 10^{-3}$), both of which restrict our discussion in the regime for 1D BECs, where Dirac dynamics instead of nonlinear dynamics dominates. In this case, the increase in particle number is achieved by proportionally increasing the length l_0 of the BEC with small γ. For comparison, we also calculate the scaling of $\langle T \rangle$ for the atom numbers of

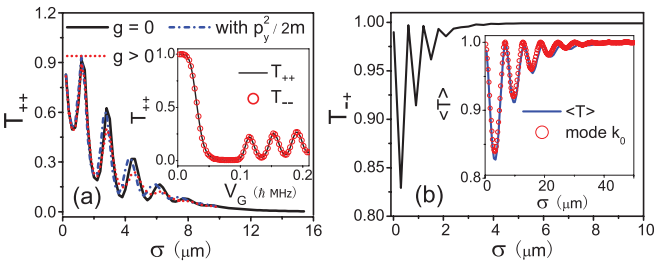

FIG. 3. (Color online) KT of BECs. (a) $T_{++}(\sigma)$ for $V_G/\hbar = 0.2$ MHz and $T_{++}(V_G)$ (inset) for $\sigma = 5$ μm. The tunnelings of a BEC with the classic kinetic energy term and the conventional atomic interaction ($N = 2 \times 10^4$, $l_\perp = 1.4$ μm, and $a_s = 5a_0$, with a_0 being the Bohr radius) are also depicted. (b) Coefficients $T_{-+}(\sigma)$, $\langle T(\sigma) \rangle$ (inset) of one atom with central mode k_0 and of 10^4 atoms for $V_G/\hbar = 0.2$ MHz. The other parameters in (a) and (b) are $l_0 = 10$ μm, $k_0 = 5.5 \times 10^5$ m^{-1}, $\gamma_z/\hbar = 30$ kHz, and $d = 4(l_0 + \sigma)$.

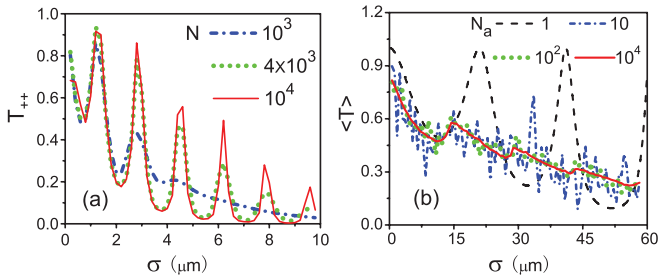

FIG. 4. (Color online) Comparison of KT of BECs with that of an ensemble of noncondensed atoms. (a) $T_{++}(\sigma)$, with $N = 10^3$, 4×10^3, and 10^4, are shown by fixing the energy $E_{\rm int}$ for $l_0 = 10$ μm and $d = 4(l_0 + \sigma)$. (b) $\langle T(\sigma) \rangle$, with $N_a = 1$, 10, 10^2, and 10^4 atoms, for $\sigma_k = 5 \times 10^5$ m^{-1}. The other parameters in (a) and (b) are $V_G/\hbar = 0.2$ MHz, $k_0 = 5.5 \times 10^5$m^{-1}, and $\gamma_z/\hbar = 30$ kHz.

1 (with $k_i = k_0$), 10, 10^2, and 10^4 in Fig. 4(b). Comparing Fig. 4(a) with Fig. 4(b), a distinct difference between the BEC and the ensemble average of the individual atoms is that the coefficient T_{++} increases with increasing atomic number of the BEC, while the coefficient $\langle T \rangle$ decreases with increasing atomic number. However, in order to keep the same interaction parameter in the above calculation, we have increased simultaneously the particle number and the width of the Gaussian wave packet. In this way the momentum distribution of the wave functions is shrunk, which is a dominant reason for the above scaling feature. That many atoms may condense into the same momentum state is essential for the observation of KT in a BEC.

V. DISCUSSION AND CONCLUSION

Before concluding, we wish to make two additional comments. (i) To judge the feasibility of the Dirac approximation in Eq. (2), the coefficients T_{++} with or without the quadratic term are compared in Fig. 3(a). It is shown that the quadratic term leads to merely a slight left-shift of the tunneling peaks. This phenomenon can be interpreted by the fact that the wavelength of the BEC inside the barrier decreases slightly in the presence of the additional low kinetic energy. This result verifies that the approximation leading to the Dirac equation is well satisfied. (ii) In Fig. 3(a), we have also calculated the transmission coefficient for BECs with conventional atomic interactions without Feshbach resonance, in which case the experimental setup can be simplified. The result shows that the effect of the realistically weak interaction is small; it merely smooths the tunneling oscillation slightly. Therefore the exotic tunneling phenomena addressed here survive in the case of weak interactions between atoms.

In summary, we have proposed an experimental scheme to detect macroscopic KT using a spin-orbit-coupled BEC. Through numerical simulations, we have elaborated that such macroscopic KT can be observed under realistic conditions. In view of the fact that a spin-orbit-coupled BEC was realized in a very recent experiment [13], it is anticipated that the present proposal will be tested in an experiment in the near-future.

ACKNOWLEDGMENTS

This work was supported by the NSFC (Grants No. 11125417, No. 10974059, No. 11104085, No. 91121023, and No. 11004065), the SKPBR (Grant No. 2011CB922104), the GRF (HKU7058//11P) and CRF of the RGC of Hong Kong.

APPENDIX: THE DERIVATION OF T(k_i) IN EQ. (8)

The Dirac equation for particle scattering by a Gaussian potential cannot be solved analytically for an incoming atom with energy $E_i = \sqrt{(\hbar v_y k_i)^2 + \gamma_z^2}$ and momentum $p_i = \hbar k_i$. However, here we adopt an efficient method to solve it numerically based on transfer matrix methods [9]. The numerical procedures are outlined as follows. First, one cuts the Gaussian potential into a spatially finite range $y \in [-y_c, y_c]$, where the cutoff position y_c should be chosen to guarantee that the potential height outside the range is low enough to be transparent for the atoms, i.e., $V_b^{\mathrm{G}}(y_c) \ll E_i, V_{\mathrm{G}}$. Second, one divides this range equally into n spindly segments, and each segment may be considered a square potential if n is large enough. The potential height of the jth ($j = 1, 2, \ldots, n$) square potential is given by $V_j = V_b^{\mathrm{G}}(y_j + f/2)$, with $y_j = -y_c + (j-1)f$ and the width of each potential $f = 2y_c/n$. In this case, the Gaussian potential can be viewed approximately as a sequence of connective small square potential barriers, and thus the transmission coefficient $T(k_i) \approx 1/|m_{11}|^2$, where m_{11} is the first element in the whole transfer matrix $M = M_n M_{n-1} \ldots M_j \ldots M_2 M_1$. Here M_j denotes the transfer matrix of the jth square potential barrier, whose explicit elements are given by [9]

$$
\begin{aligned}
(M_j)_{11} &= \left(\cos\frac{p_j f}{\hbar} + i\frac{\kappa^2 + \kappa_j^2}{2\kappa\kappa_j} \sin\frac{p_j f}{\hbar} \right) e^{-\frac{i}{\hbar} p_i f}, \\
(M_j)_{12} &= \left(i\frac{\kappa_j^2 - \kappa^2}{2\kappa\kappa_j} \sin\frac{p_j f}{\hbar} \right) e^{-\frac{i}{\hbar} p_i (y_j + y_{j+1})}, \\
(M_j)_{21} &= (M_j)_{12}^*, \quad (M_j)_{22} = (M_j)_{11}^*,
\end{aligned}
\tag{A1}
$$

where $\kappa = (E_i - \gamma_z)/(v_y p_i)$ and $\kappa_j = (E_i - \gamma_z - V_j)/(v_y p_j)$, with $(E_i - V_j)^2 = v_y^2 p_j^2 + \gamma_z^2$. Note that this numerical calculation scheme recovers the nonrelativistic scattering governed by the Schrödinger equation.

[1] O. Klein, Z. Phys. **53**, 157 (1929).
[2] N. Dombey and A. Calogeracos, Phys. Rep. **315**, 41 (1999).
[3] M. I. Katsnelson, K. S. Novoselov, and A. K. Geim, Nature Phys. **2**, 620 (2006); V. Jakubsky, L. M. Nieto, and M. S. Plyushchay, Phys. Rev. D **83**, 047702 (2011).
[4] L. Lamata, J. León, T. Schätz, and E. Solano, Phys. Rev. Lett. **98**, 253005 (2007).
[5] R. Gerritsma, G. Kirchmair, F. Zahringer, E. Solano, R. Blatt, and C. F. Roos, Nature (Landon) **463**, 68 (2010); R. Gerritsma, B. P. Lanyon, G. Kirchmair, F. Zahringer, C. Hempel, J. Casanova, J. J. Garcia-Ripoll, E. Solano, R. Blatt, and C. F. Roos, Phys. Rev. Lett. **106**, 060503 (2011).
[6] S. L. Zhu, B. Wang, and L. M. Duan, Phys. Rev. Lett. **98**, 260402 (2007); I. I. Satija, D. C. Dakin, J. Y. Vaishnav, and C. W. Clark, Phys. Rev. A **77**, 043410 (2008); C. Chamon, C.-Y. Hou, R. Jackiw, C. Mudry, S.-Y. Pi, and G. Semenoff, Phys. Rev. B **77**, 235431 (2008).
[7] J. Ruseckas, G. Juzeliunas, P. Ohberg, and M. Fleischhauer, Phys. Rev. Lett. **95**, 010404 (2005); S. L. Zhu, H. Fu, C. J. Wu, S. C. Zhang, and L. M. Duan, *ibid.* **97**, 240401 (2006).
[8] J. Y. Vaishnav and C. W. Clark, Phys. Rev. Lett. **100**, 153002 (2008); G. Juzeliūnas, J. Ruseckas, M. Lindberg, L. Santos, and P. Öhberg, Phys. Rev. A **77**, 011802(R) (2008).
[9] S. L. Zhu, D. W. Zhang, and Z. D. Wang, Phys. Rev. Lett. **102**, 210403 (2009).
[10] N. Stander, B. Huard, and D. Goldhaber-Gordon, Phys. Rev. Lett. **102**, 026807 (2009).

[11] A. F. Young and P. Kim, Nature Phys. **5**, 222 (2009).
[12] T. D. Stanescu, B. Anderson, and V. Galitski, Phys. Rev. A **78**, 023616 (2008); C.-J. Wang, C. Gao, C.-M. Jian, and H. Zhai, Phys. Rev. Lett. **105**, 160403 (2010); T. L. Ho and S. Zhang, e-print arXiv:1007.0650.
[13] Y. J. Lin, K. Jimenez-Carcia, and I. B. Spielman, Nature (London) **471**, 83 (2011).
[14] X.-J. Liu, M. F. Borunda, X. Liu, and J. Sinova, Phys. Rev. Lett. **102**, 046402 (2009); C. Zhang, Phys. Rev. A **82**, 021607(R) (2010).
[15] M. Merkl, A. Jacob, F. E. Zimmer, P. Öhberg, and L. Santos, Phys. Rev. Lett. **104**, 073603 (2010).
[16] M. G. Tarallo, J. Miller, J. Agresti, E. D'Ambrosio, R. DeSalvo, D. Forest, B. Lagrange, J. M. Mackowsky, C. Michel, J. L. Montorio, N. Morgado, L. Pinard, A. Remilleux, B. Simoni, and P. Willems, Appl. Opt. **46**, 26 (2007).
[17] L. Khaykovich, F. Schreck, G. Ferrari, T. Bourdel, J. Cubizolles, L. D. Carr, Y. Castin, and C. Salomon, Science **296**, 1290 (2002).
[18] N. Dombey, P. Kennedy, and A. Calogeracos, Phys. Rev. Lett. **85**, 1787 (2000).
[19] J. Larson and E. Sjoqvist, Phys. Rev. A **79**, 043627 (2009), and references therein.
[20] D. S. Petrov, G. V. Shlyapnikov, and J. T. M. Walraven, Phys. Rev. Lett. **85**, 3745 (2000).